Journal of Applied Polymer Science

Adaptability of a Hydrophobically Associating Polyacrylamide/Mixed-Surfactant Combination Flooding System to the Shengli Chengdao Oilfield

Xin-Min Zhang,[1,2] Yong-Jun Guo,[1,2] Jian-Xin Liu,[3] Yang-Wen Zhu,[4] Jun Hu,[2] Ru-Sen Feng,[1] Chun-Yan Fu[2]

[1]State Key Laboratory of Oil and Gas Reservoirs Geology and Exploration, Southwest Petroleum University, Chengdu, Sichuan 610500, China

[2]Sichuan Guangya High-Tech Company, Limited, Nanchong, Sichuan 637001, China

[3]Petroleum Engineering College, Yangtze University, Wuhan 430100, China

[4]Geology Scientific Research Institute, Sinopec Shengli Oilfield Company, Dongying 257015, China

Correspondence to: X.-M. Zhang (E-mail: kaixin20@126.com) or Y.-J. Guo (E-mail: gyfzgyj@126.com)

ABSTRACT: We investigated the performance of a combination flooding system composed of hydrophobically associating polyacrylamide (HAPAM) and a mixed surfactant [fatty acid disulfonate anionic gemini surfactant (DMES) plus the nonionic surfactant Triton X-100 (TX-100)] under the reservoir conditions of the Shengli Chengdao oilfield. With 1800 mg/L HAPAM and 300–3000 mg/L mixed surfactant, the surfactant–polymer (SP) flooding system reached an ultralow oil–water interfacial tension, and the viscosity of the system was greater than 40 mPa s. After the solution was aged for 120 days, its viscosity was still more than 40 mPa s; this indicated a good aging stability. The core flooding experiments with different porous media permeabilities showed that the SP flooding system created a higher resistance factor and residual resistance factor. In addition, the indoor flooding experiments indicated that the SP combination flooding system increased the enhanced oil recovery by more than 30% over that of the original oil in place compared with the water flooding system. Therefore, it was feasible to use an SP flooding system in the Chengdao oilfield. © 2014 Wiley Periodicals, Inc. J. Appl. Polym. Sci. **2014**, *131*, 40390.

KEYWORDS: aging; oil and gas; surfactants

Received 18 July 2013; accepted 1 January 2014
DOI: 10.1002/app.40390

INTRODUCTION

The Shengli Chengdao oilfield is located in the shallow waters of the South Bohai Sea and was put into production in 1993. Because of its highly heterogeneous sandstone, poor connectivity, and the complex relationship between the oil and water phase,[1] its resources have been used with a low oil production rate and a low degree of recovery since its exploration. Therefore, it is necessary to develop some effective methods for increasing its oil production rate and recovery degree.

Recently, chemical flooding has been widely and successfully used in enhanced oil recovery (EOR).[2–6] Experiments indoors and in oilfields have shown that alkali–surfactant–polymer (ASP) flooding can increase the oil recovery factor by 20% over that of water flooding or polymer flooding. However, the preparation water (made of seawater and well water) in the Chengdao Oilfield has high levels of calcium and magnesium ions, so the rich alkalis in ASP flooding may react with these divalent ions to produce precipitates, and this could lead to difficult problems, such as the serious scaling of the production well wellbore and a decrease in the formation permeability.[7,8] At the same time, the alkali can cause adverse effects on the matching properties of the polymer and surfactant,[9–14] and this limits the application of the ASP flooding technology.[13,14] Fortunately, there is no alkali in the surfactant–polymer (SP) system, so the unfavorable factors of ASP flooding mentioned previously can be avoided with this system. As a result, the swept volume and wash-oil efficiency can be greatly improved, and the SP system can be considered as a viable method to improve the oil recovery.[15,16]

There are some literature reports on SP systems, and partially hydrolyzed polyacrylamide is usually adopted as the tackifier.[16–18] However, the popularization and application of partially hydrolyzed polyacrylamide is greatly limited because of its poor

temperature resistance and salt resistance, easy breaking of the molecular chain, and the sharp, unrecoverable decrease in the viscosity during pump priming.[19,20] Hydrophobically associating polyacrylamide (HAPAM) is a class of water-soluble polymers containing a small amount of hydrophobic groups or chains. The hydrophobic groups or chains have a unique amphiphilic structure, and this makes the solution characteristics quite different from those of general water-soluble polymers.[21,22] When the solution concentration above the critical association concentration forms in a space network structure based on supermolecular intermolecular association, the addition of salt will enhance the hydrophobic association so that the viscosity of the solution will remain stable or even increase. This indicates that it has better thickening properties, temperature resistance, salt resistance, shear resistance, and stability compared with hydrolyzed polyacrylamide.[23–25]

Generally speaking, the SP system has a higher requirement for surface-active agents, and under alkali-free conditions, it is very difficult for the surface-active agent to make the oil–water interface tension reach 10^{-3} mN/m.[26–28] Petroleum sulfonate surfactants have been used in ASP and SP flooding systems, presumably because of their high oil–water interfacial activity. However, the stable supply of petroleum sulfonates with adequate quality is problematic because raw materials possess substantial composite differences, and this naturally complicates the production technology.[29] So, the development of new surfactants with higher interfacial activities and wider suitabilities becomes an important target in obtaining an SP flooding system in practical applications. Through a linking group, the two conventional surfactants in the hydrophilic head group or close to the hydrophilic head group are joined together to form a new class of surfactant, the gemini surfactant, which has strong potential because of its demonstrated critical micelle concentration, temperature resistance, salt resistance, high surface activity,[30–32] and good wetting properties.

It has been found that the hydrophobic modification of water-soluble polymers can lead to characteristic changes in their interaction with surfactants, especially in terms of their rheological properties. Under the conditions of lower surfactant concentrations, hydrophobic groups are surrounded by a large number of micelles; this consequently reduces the amount of hydrophobic groups in hydrophobic domains, alleviates hydrophobic interactions, and affords a sharply decreasing apparent viscosity.[33,34] In addition, some studies have demonstrated that the properties of SP solutions can be modulated with mixed surfactants. For example, it has been found that cosurfactants with appropriate hydrophilic–lipophilic balances, such as nonylphenol ethoxylates, can be used to mitigate disadvantageous effects.[35,36]

In this study, we mainly investigated the properties of the sulfonate gemini surfactant and HAPAM under the reservoir conditions of the Shengli Chengdao oilfield. Through their combination, we obtained an SP system containing a gemini-surfactant-based mixed surfactant and HAPAM, and the overall performance of the system was studied to determine the feasibility of the combination flooding system in the Shengli Chengdao oilfield.

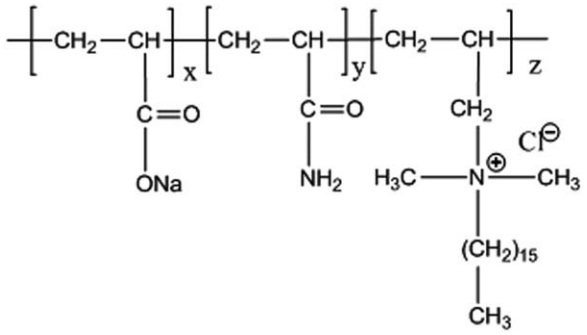

Figure 1. Structure of HAPAM.

EXPERIMENTAL

Materials

HAPAM was polymerized according to ref. 37 (molecular weight = 18.5×10^6, degree of hydrolysis = 25.3%, hydrophobic monomer molar content = 0.18%), and the structural formula is shown in Figure 1. According to Chen's patent,[38] the sulfonate gemini surfactant DMES was prepared, and the structural formula is shown in Figure 2. Octyl phenol polyoxyethylene ether (TX-100) was purchased from Chengdu Kelong Chemical Reagents, Ltd., and degassed oil with a density of 0.95 g/cm^3 was provided by Geology Scientific Research Institute of the Shengli Oilfield.

Preparation of the Surfactant and Polymer Solutions

To prepare the surfactant solution, the surfactant was diluted to the target concentration with injected water at room temperature.

To prepare the polymer solution, HAPAM was completely dissolved in the injected water at 45°C to prepare a 5000 mg/L stock solution, and then, we diluted the polymer to the target concentration using the injected water.

To prepare the SP flooding system, we added the polymer and surfactant solution to a beaker with the injected water and mixed it well at a constant agitation speed.

The injected water was #3 water unless otherwise specified.

Measurement of the Viscosity. The viscosity of the solution was measured with a Brookfield DV-III viscosity meter (American Brookfield Co.) at a shear rate of 7.34 s^{-1} at 65°C (special request excluded).

Measurement of the Oil–Water Interfacial Tension (IFT). The oil–water IFTs between the solution and crude oil were measured with a Texas-500C spinning drop tension meter (Bowing) at 65°C, which could automatically record the IFT by an image pickup device and image acquisition software.

Measurement of the Shear Stability. A capillary with a length of 20 cm and a diameter of 0.14 cm was connected to the

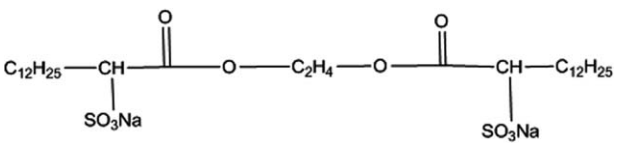

Figure 2. Structure of the DMES gemini surfactant.

bottom of a cylindrical stainless steel container with volume of 500 mL. Then, the SP solution was put into the container, and its pressure was kept at 0.1 MPa by high-pressure nitrogen. Afterward, the valve at the bottom of the container was opened and the solution was sheared with the capillary flow into the beaker. During the process, the original and final viscosities of the solution were measured.

Aging Stability. We injected 40 mL of SP solution into each of the eight ampules and then removed the oxygen in the bottles with nitrogen. Afterward, we sealed the bottles and put them in a 65°C oven. At regular intervals, we tested the solution viscosity and oil–water IFT.

Resistance Factor (RF) and Residual Resistance Factor (RRF).

1. Cores with a diameter of 2.5 cm and a length of 10 cm were dried at 80°C for 24 h, and then, they were put into the beaker and saturated with the injected water under *in vacuo* conditions. Their dry weight and wet weight were measured, and the difference was the pore volume (PV; 1 PV).
2. The saturated cores were inserted into the core holders and put into a multifunction-displacement device (Haian Oil Instrument Co.), and then, the brine was injected at a speed of 0.5 m/day at 65°C until the pressure stabilized. The water-flooding pressure drop (ΔP_{wb}) was recorded, and the permeability was measured according to Darcy's law.
3. An SP solution of 3 PV was injected under normal conditions, the SP-flooding pressure drop (ΔP_{SP}) was recorded, and the RF was calculated according to eq. (1). Then, the brine was injected until the pressure stabilized, the pressure drop of the subsequent water flooding (ΔP_{wa}) was obtained, and the RRF was calculated according to eq. (2):

$$RF = \frac{(\Delta P)_{SP}}{(\Delta P)_{wb}} \quad (1)$$

$$RRF = \frac{(\Delta P)_{wa}}{(\Delta P)_{wb}} \quad (2)$$

EOR.

1. The artificial nonhomogeneous square cores (side length = 4.5 cm, length = 30 cm, and high, medium, and low permeabilities = 2, 1, and 0.5 μm^2, respectively) were inserted into the core holders, and the water permeability and PV values were measured with the method mentioned earlier were corrected.
2. The crude oil was injected into the cores to saturate the oil, and the oil ratio in the produced fluid was measured every 10 min until the instantaneous oil ratio was above 98%. The original oil saturation was calculated by virtue of the proportion of crude oil volume in the core and PV. Notably, the cores were placed for 16 h to reach oil–water balance.
3. The constant-flux pump was turned on to start the first water flooding, and the volumes of the oil and water in the produced fluid were recorded every 10 min. Water flooding was stopped until the instantaneous water cut was above 98% for five consecutive points, and then, the water flooding recovery was obtained.
4. The SP solution of 0.3 PV was injected until the water cut was above 98%, and then, the SP flooding recovery could be calculated.
5. We continue the water flooding until the water cut was above 98%, and then, the subsequent water flooding recovery could be calculated. The sum of the recovery of SP flooding and subsequent water flooding showed an improvement in the oil recovery.

RESULTS AND DISCUSSION

Properties of the Surfactant

Solubility of the Surfactant. The application of a surfactant was directly affected by its solubility in brine. The solubility behavior of DMES in water indicated that there was no insoluble substance within its application concentration scope (<5%).

Effect of the Temperature on IFT. A series of surfactant solutions (100–3000 mg/L) was prepared, and then, the temperature resistance was investigated by the testing of the oil–water IFT at 45, 65, and 85°C, respectively. As Figure 3 shows, the oil–water IFTs of the solution reached an ultralow value ($<1.0 \times 10^{-2}$ mN/m) under wider experimental conditions.

The gemini surfactant had a good interfacial activity because of the chemical bonding between the two ion head bases so that both ends of the two surfactant molecules shortened the distance to strengthen the hydrophobic binding force of the carbon–hydrogen bonds. This greatly weakened the electrostatic repulsion between the ion head bases and made the surface arrangement more close in water.[39,40] As shown in Figure 3, the temperature had no big influence on the surface activity of the surfactant in the range of researched temperatures (45–80°C). This indicated that the surfactant could adapt to a wide range of reservoir temperatures.

Effect of the Salinity on IFT. Electrolytes usually have an obvious effect on the interfacial behavior of surfactants by changing not only the form of the surfactant molecules in solution but also their distribution in oil–water. Therefore, it was necessary to consider the influence of salinity on the oil–water

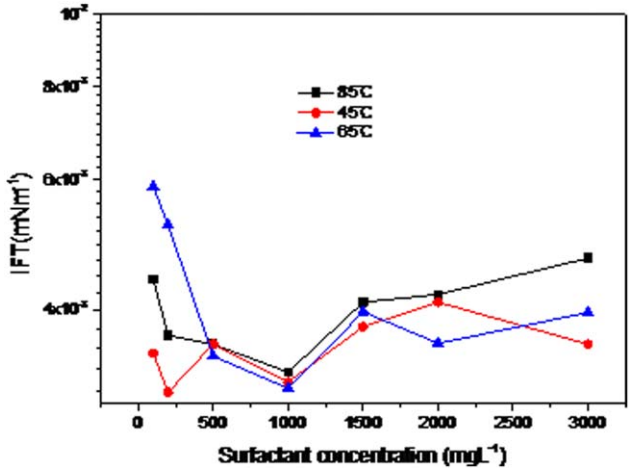

Figure 3. IFT versus the DMES concentration at different temperatures (Shengli #3 water and Shengli oil). [Color figure can be viewed in the online issue, which is available at wileyonlinelibrary.com.]

Table I. Main Components of the Experimental Water for the Shengli Injected Water

	Ion content (mg/L)			
Ion	Well water (#1)	Seawater (#2)	2:1 well water/seawater (#3)	1:2 well water/seawater (#4)
$K^+ + Na^+$	3,468	9,369	5,435	7,404
Ca^{2+}	64	417	183	299
Mg^{2+}	17	1,160	398	779
Cl^-	5,217	17,703	9,379	13,545
SO_4^{2-}	48	1,035	377	706
HCO_3^-	445	174	355	264
Total salinity	9,259	29,858	16,127	22,999

IFT in the oil-displacement system. At the same time, to conserve freshwater resources and increase the suitability of the displacement system to the injected water (the main components are shown in Table I), the solution preparation in the Shengli offshore oilfield needs to reduce the proportion of well water and increase that of seawater.

Figure 4 shows that the oil–water IFTs decreased slightly with increasing mineralization degree. The addition of the inorganic salt made the electrostatic repulsion of the gemini surfactant decrease and led to the formation of micelles in the molecular thermodynamic movement state; this increased the interfacial activity.[41] In the measurement range, the oil–water IFTs could reach an ultralow value, and this meant that the surfactant had ideal interfacial activity in the researched range of salinity.

Polymer Properties

Relationship of the Viscosity and the Concentration. The HAPAM solution was diluted from 500 to 2000 mg/L to measure the solution viscosity, and the data are shown in Figure 5. The results show that the HAPAM had a good viscosity-increasing capacity because of polymer-chain enwinding and an associative effect, and the viscosity increased with the increasing concentration of the solution. When the concentration of the polymer solution reached above 1750 mg/L, the viscosity was higher than 40 mPa s.

Polymer Solution Viscosity Changes with Temperature. As Figure 6 shows, the viscosity of the polymer solution decreased slightly with increasing temperature. Because the associative effect was an entropy-driven process, it was strengthened with the increase in the temperature. Furthermore, the temperature rise enhanced the thermodynamic movement of the ionic groups and extended the molecular chains; this was conducive to intermolecular association. Thus, the spatial network structure formed in the solution mainly in the form of noncovalent bond association and increased the structural viscosity,[42] which slowed down the decreasing trend of the viscosity.

Polymer Solution Viscosity Changes with Mineralization Degree. The viscosity of the polymer solution decreased slightly with increasing mineralization degree and still reached 39.5 mPa s with a salinity of 29,858 mg/L (seawater). The addition of salt to the solution enhanced the solvent's polarity and impelled the hydrophobic groups to contact with the minimum water volume by further enhancing the intermolecular hydrophobic association; this correspondingly increased the physical crosslinking points of the macromolecular clew. Thus, the intermolecular association ability and hydrodynamic volume were enhanced, and a significant rise in the solution viscosity occurred.[43] This consequently weakened the adverse effects of the polymer molecular chain curl.

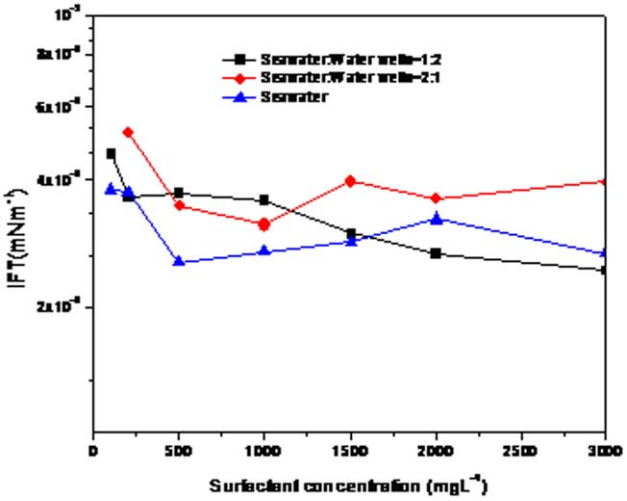

Figure 4. IFT versus the DMES concentration for different degrees of mineralization (65°C and Shengli oil). [Color figure can be viewed in the online issue, which is available at wileyonlinelibrary.com.]

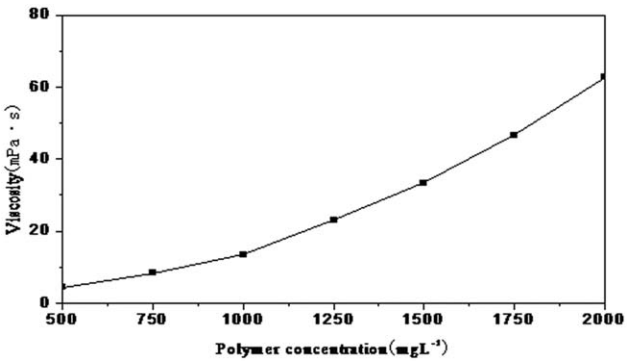

Figure 5. Viscosity versus C_{HAPAM} (Shengli #3 water and 65°C).

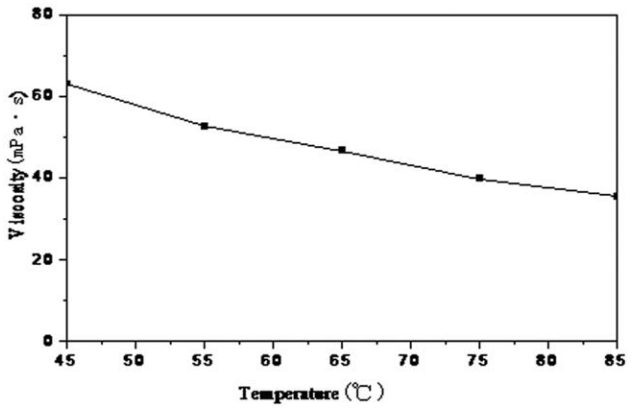

Figure 6. Viscosity of HAPAM at different temperatures (C_{HAPAM} = 1800 mg/L, 65°C, and Shengli #3 water)

System Construction of Compound Flooding

In chemical flooding, the viscosity and IFT are two most important parameters affecting the displacement efficiency. In this part of the study, to build a higher performance displacement system, we added DEMS to a HAPAM solution with concentration of 1800 mg/L and obtained an SP flooding system for the Shengli Chengdao oilfield with formula optimization.

Effect of the Cosurfactant on the Viscosity and IFT. As shown in Figure 7, when a little DMES was added to the HAPAM solution without cosurfactant, physical crosslinking formed through a bridge effect between the surfactant and hydrophobic group of HAPAM; this led to a rapid increase in the viscosity. However, excessive surfactant in the solution could destroy the bridge because of the wrapping of hydrophobic groups with surfactant molecules; this weakened the associative effect between different polymer chains and finally led to a sharp decline in the viscosity.[33,34] As reported in the literature, cosurfactants such as nonionic surfactants can significantly increase the viscosity and ease disadvantageous effects, especially under the conditions of high surfactant concentrations.[35,36] After screening a number of different cosurfactants, we found that teroctylphenoxy polyoxyethanol (TX-100) could dampen the

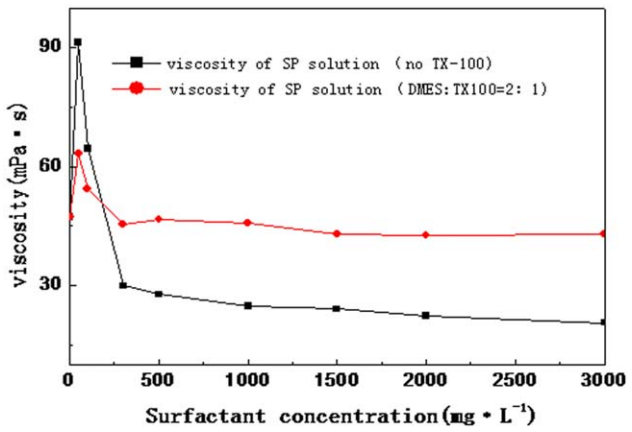

Figure 7. Viscosity of the SP system versus the surfactant concentration (C_{HAPAM} = 1800 mg/L, 65°C, Shengli #3 water, and Shengli oil). [Color figure can be viewed in the online issue, which is available at wileyonlinelibrary.com.]

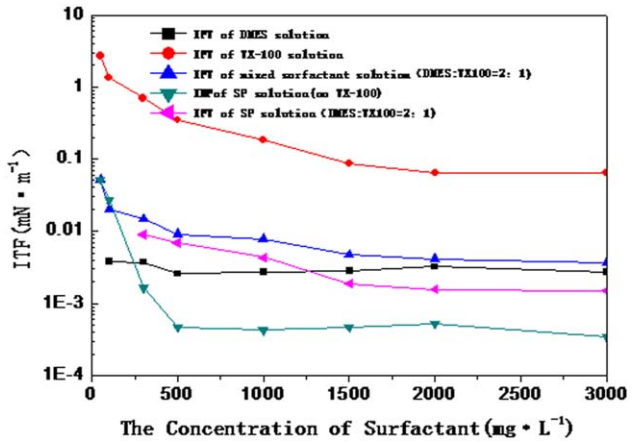

Figure 8. IFT of the SP system versus the surfactant concentration (C_{HAPAM} = 1800 mg/L, 65°C, Shengli #3 water, and Shengli oil). [Color figure can be viewed in the online issue, which is available at wileyonlinelibrary.com.]

decrease in viscosity and accelerate the surfactant concentration window of increasing viscosity. Notably, the addition of TX-100 to the micellar solutions of anionic surfactants increased the microviscosity of the micellar interface, and the TX-100 molecules were able to penetrate through the DMES-14 micelles, which certainly decreased the micellar charge density and resulted in a closer arrangement of long hydrophobic chains.[44]

Furthermore, we compared the IFTs of five systems (Figure 8) and found that there was synergism in the IFT and the DMES-14 reduction effectiveness with HAPAM. However, the HAPAM solution without surfactant did not obviously decrease the IFT, perhaps because the HAPAM stabilized the oil–water emulsion.[45,46] The strong network structure of HAPAM was able to hold oil particles without the occurrence of phase inversion and played a vital role in this SP system. Although the IFT of the solution increased with the addition of TX-100, it still reached ultralow values.

Impact of the Proportion of DMES and TX-100 on the Performance. The DMES and TX-100 were mixed in ratios from 3:4 to 4:1 (w/w), and their impacts on the performance of the SP system are shown in Figures 9 and 10. When the ratio was greater than 1.5 and the surfactant concentration was above 300 mg/L, the oil–water IFTs of the SP system reached 10^{-3} mN/m. In a larger ratio range, the viscosity of the SP system was higher than 40 mPa s. According to the results, we obtained the optimal formulation of the combination flooding system with concentrations of HAPAM, DMES, and TX-100 of 1800, 2000, and 1000 mg/L, respectively.

Performance of the Combination Flooding System

Shear Resistance of the SP Flooding System. Before the solution of the SP combination system was injected into the deep reservoir, it had to flow through the borehole formation in the well bottom, which had a small flow area, a large flow rate, and a high pore velocity. The polymers of the SP combination system solution were bound to be influenced by high-speed borehole shearing; this affected the viscosity of the whole combination system. Therefore, it was necessary to study the shear resistance of the combination system solution.

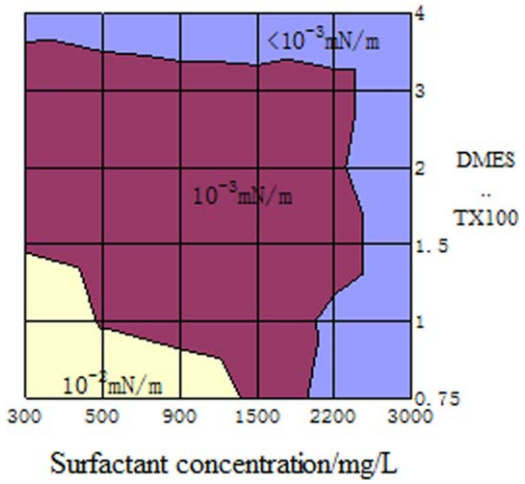

Figure 9. IFT versus the surfactant concentration with different proportions of DMES-14 and TX-100 (C_{HAPAM} = 1800 mg/L, 65°C, Shengli #3 water, and Shengli oil). [Color figure can be viewed in the online issue, which is available at wileyonlinelibrary.com.]

After capillary shearing, the viscosity of the SP combination system decreased from 47.5 mPa s before shearing to 45.6 mPa s, and the viscosity retention rate reached 96%. At the same time, its IFT did not change. The results indicate that the combination system had a good shear resistance. In the associative polymer solution, the polymer molecules formed intramolecular and intermolecular associative structures with weak interaction, and the structures were reversible structures. Because of the relatively low molecular weight of the associative polymer, the shear force could not break the chain structure but only most associative structures. When the shear force disappeared, these associative structures recovered, and the viscosity of the solution increased.[23,25,47]

Aging Stability of the SP Flooding System. In practice, it often takes a few months for the SP flooding system to be extracted

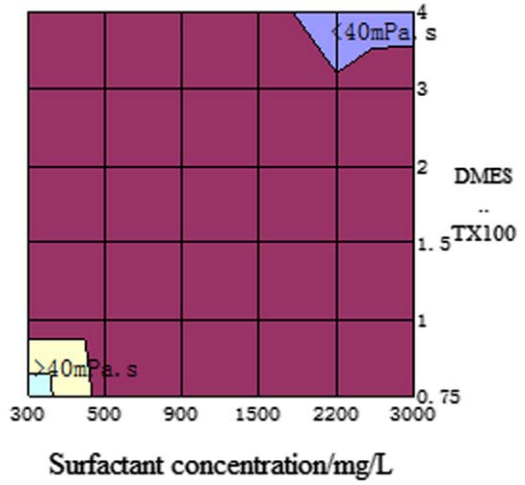

Figure 10. Viscosity versus the surfactant concentration with different proportions of DMES and TX-100 (C_{HAPAM} = 1800 mg/L, 65°C, Shengli #3 water, and Shengli oil). [Color figure can be viewed in the online issue, which is available at wileyonlinelibrary.com.]

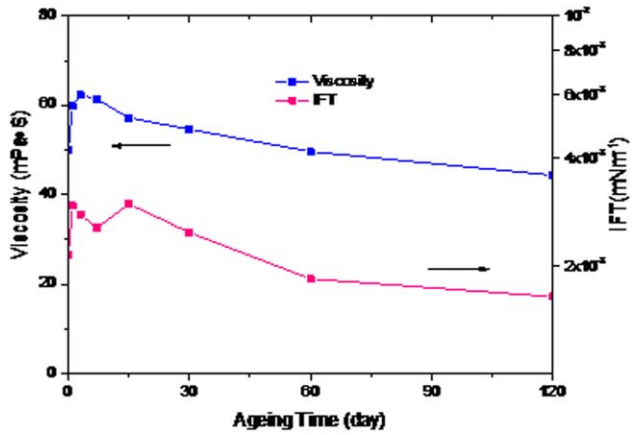

Figure 11. Viscosity and IFT of the SP system versus the aging time [C_{HAPAM} = 1800 mg/L, C_s = 3000 mg/L (DMES/TX-100 = 2:1), 65°C, Shengli #3 water, and Shengli oil]. [Color figure can be viewed in the online issue, which is available at wileyonlinelibrary.com.]

after it is injected into the formation, so the combination system should have a good thermal stability.

The complete dissolution of the polymer makes the molecular chain entirely extended so that the viscosity of the system increases.[48] Then, because of oxidation and thermal degradation, the viscosity of the system slightly decreases. As Figure 11 shows, the viscosity of this SP system first increased and then decreased with time. However, after 120 days of aging, the viscosity was still greater than 40 mPa s. When we measured the oil–water IFT, it showed no great change over time and was basically at 1–3 × 10^{-3} mN/m. Therefore, the system had a good aging stability.

RF and RRF. During the flow process of the SP flooding system, polymer molecules in the reservoir pore, mechanical trapping, chemical adsorption, and retention effect resulted in a decrease in the porous media permeability while the flow resistance increased. As for a given reservoir, the higher the RF is, the stronger the capacity to improve the mobility ratio of the displacement fluid becomes; this is helpful for improving the reservoir swept volume and oil recovery amplitude. In addition, the higher RRF means a greater decrease in the porous media permeability, and the chance of enhancing the oil recovery magnitude is higher in subsequent water flooding.[49,50]

Figure 12 shows that the injection pressure of the SP system in the lower permeability media injection process first increased and then remained stable with injection volume and that there was no indication of pressure clogging with a dramatic increase; this proved that the system had a good injection performance. As shown in Table II, the SP flooding system with different porous media permeability obtained a higher RF and RRF. This indicated that the system had a good capacity to control the mobility so that the recovery in SP flooding and subsequent water flooding could be improved significantly.

Flooding Recovery of the Combination Flooding System. Three heterogeneous cores were used to study the flooding capacity of the combination flooding system. As shown in

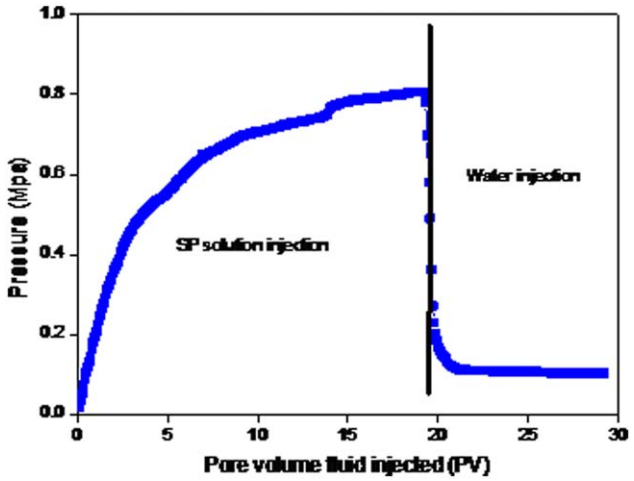

Figure 12. Relationship of the injection volume of the SP solution and the pressure in a porous medium [C_{HAPAM} = 1800 mg/L, C_s = 3000 mg/L (DMES/TX-100 = 2:1), 65°C, Shengli #3 water, and permeability = 0.21 μm^2]. [Color figure can be viewed in the online issue, which is available at wileyonlinelibrary.com.]

Table III and Figure 13, the combination flooding system enhanced the oil recovery by 30% or more based on water flooding and 6% more than the separate polymer flooding. At the same time, the decrease in IFT made most of the residual oil in cores active and displaced it out; this played a decisive role in enhancing the microscopic oil-displacement efficiency. When the oil–water IFT decreased from 10 to 10^{-2} mN/m, the recovery value increased greatly. However, when the IFT decreased from 10^{-2} to 10^{-3}mN/m, the increasing magnitude of the flooding recovery was very small, and the method of enhancing the microscopic oil-displacement efficiency by reducing the oil–water IFT has very limited potential.[51–53]

Table II. RF and RRF for the SP Systems with Different Permeability Cores

Number	Porosity (%)	Water permeability (10^{-3} μm^2)	RF	RRF
1	31	210	347.6	36.6
2	30.9	532	231.6	37.4
3	31.7	974	168.3	22.4
4	31.4	1549	89.4	18.9

Homogeneous square cores (diameter = 2.5 mm, length = 10 cm).

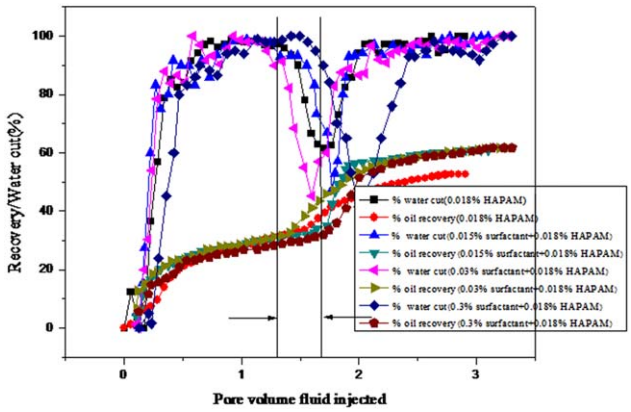

Figure 13. Cumulative oil recovery and water cutting of the SP flooding with IFT (nonhomogeneous permeability cores; 0.3 PV and 65°C). [Color figure can be viewed in the online issue, which is available at wileyonlinelibrary.com.]

CONCLUSIONS

1. The evaluation of the temperature resistance and salt resistance of DMES and HAPAM showed that DMES had good interfacial activity, solubility, temperature resistance, and salt tolerance and that HAPAM had a good capacity for thickening and good salt resistance to calcium and magnesium ions.
2. By investigating the interaction between DMES/TX-100 and HAPAM, we obtained a suitable formulation for a combination flooding system for offshore heavy oil reservoirs in the Shengli Chengdao oilfield with a concentration of hydrophobically associating polyacrylamide (C_{HAPAM}) of 1800 mg/L, a C_s (the concentration of surfactants) of 300–3000 mg/L, and a DMES/X-100 ratio of 2:1 (w/w).
3. The composite surfactant at concentrations of greater than 300 mg/L reduced the Shengli offshore crude oil–water IFT to 10^{-3} mN/m, whereas the viscosity of the system remained above 40 mPa s. In addition, it had good shear resistance and aging stability, which could create a higher RF and RRF and improve the recovery ratio by above 30% on the basis of water flooding.

Table III. Oil Recovery of the SP System

Number	Porosity (%)	C_s (%)	Solution viscosity (mPa s)	IFT (mN/m)	Oil saturation (%)	Oil recovery (% original oil in place)	
						Water flooding	SP and subsequent water flooding
5	23.2	0	48.3	10	75.7	29.8	23.8
6	22.2	0.015	48.6	0.0417	75.9	30.3	30.6
7	22.5	0.03	47.3	0.00871	76.2	30.1	31.5
8	22.8	0.3	47.5	0.00242	75.6	29.6	32.1

There was a nonhomogeneous square core (height = 4.5 cm, width = 4.5 cm, length = 30 cm, permeability = 2, 1, or 0.5 μm^2).

ACKNOWLEDGMENTS

This work was carried out as a part of the National Science and Technology Major Project of China (contract grant number 2011ZX05011-004). The authors are grateful for the financial support.

REFERENCES

1. Liu, Z. J. The Petrogeologic Characteristics and Reservoir Prediction of the Upper Formation of Guantao Group in Chengdao Oilfield; Ocean University of China: Qingdao, China, **2003**.
2. Sabhapondit, A.; Borthakur, A.; Haque, I. *Energy Fuels* **2003**, *17*, 683.
3. Wang, D. M.; Dong, H. Z.; Lv, C. S.; Fu, X. F.; Nie, J. *SPE Reservoir Eval. Eng.* **2009**, *12*, 470.
4. Shutang, G.; Qiang, G. Presented at the SPE EOR Conference at Oil Gas West Asia, Muscat, Oman, April **2010**.
5. Zhou, W.; Zhang, J.; Han, M.; Xiang, W. T.; Feng, G. Z.; Jiang, W.; Sun, F. J.; Zhou, S. W.; Guo, Y. J.; Ye, Z. B. Presented at the International Petroleum Technology Conference, Dubai, United Arab Emirates, Dec **2007**.
6. Hernandez, C.; Chacon, L. J.; Anselmi, L.; Baldonedo, A.; Qi, J.; Dowling, P. C.; Pitts, M. J. *SPE Reservoir Eval. Eng.* **2003**, *6*, 147.
7. Bataweel, M.; Nasr-El-Din, H. Presented at the SPE International Symposium on Oilfield Chemistry, The Woodlands, TX, April **2011**.
8. Jiang, J. S. Enhanced Oil Recovery Technology; Petroleum Industry Press: Beijing, **2007**.
9. Sun, J.; Sun, L.; Liu, W.; Liu, X.; Li, X.; Shen, Q. *Colloids Surf. A* **2008**, *315*, 38.
10. Samanta, A.; Ojha, K.; Mandal, A. *Energy Fuels* **2011**, *25*, 1642.
11. Niu, R. X.; Cheng, J. C.; Long, B.; Li, B. L.; Zhang, C. B. *XinJiang Pet. Geol.* **2006**, *27*, 733.
12. Hou, J.; Ziu, Z.; Yue, X.; Xia, H. Presented at the SPE Annual Technical Conference and Exhibition, New Orleans, LA, **2001**.
13. Han, W.; Chen, P. Y.; Wang, S. D.; Zhang, W. G. *Oilfield Chem.* **1996**, *13*, 248.
14. SuMin, T. L. *Pet. Geol. Oilfield Dev. Daqing* **2005**, *24*, 81.
15. Liao, G. Z.; Yang, Z. Y.; Liu, Y. *Pet. Geol. Oilfield Dev. Daqing* **2001**, *20*, 40.
16. Wang, H. Y.; Cao, X. L.; Zhang, J. C.; Zhang, A. M. *J. Pet. Sci. Eng.* **2009**, *65*, 45.
17. Samanta, A.; Ojha, K.; Sarkar, A.; Mandal, A. *Adv. Pet. Explor. Dev.* **2011**, *2*, 13.
18. Cui, Z.-G.; Du, X.-R.; Pei, X.-M.; Jiang, J.-Z.; Wang, F. *Surfactants Deterg.* **2012**, *15*, 685.
19. Morgan, S. E.; McCormick, C. L. *Prog. Polym. Sci.* **1990**, *15*, 103.
20. Seright, R. S.; Seheult, M.; Talashek, T. *SPE Reservoir Eval. Eng.* **2009**, *12*, 783.
21. Ma, X.; Wang, X.; Wang, J.; Guo, D.; Wang, Y.; Ye, J.; Wang, Z.; Yan, H. *Langmuir* **2004**, *20*, 5679.
22. Cram, S. L.; Brown, H. R.; Spinks, G. M.; Hourdet, D.; Creton, C. *Macromolecules* **2005**, *38*, 2981.
23. Le Meins, J. F.; Tassin, J. F. *Macromolecules* **2001**, *34*, 2641.
24. Cao, B. G.; Dai, Q.; Chen, D. Z.; Zhang, H. J.; Zhao, Y. G. *Drilling Prod. Technol.* **2007**, *30*, 121.
25. Vittadello, S. T.; Biggs, S. *Macromolecules* **1998**, *31*, 7691.
26. Guo, W. K.; Yang, Z. Y.; Wu, X. L.; Zhang, G. Y.; Wang, H. F. *Acta Pet. Sinica* **2006**, *27*, 75.
27. Cui, Z.-G.; Du, X.-R.; Pei, X.-M.; Jiang, J.-Z.; Wang, F. *Surfactants Deterg.* **2012**, *15*, 685.
28. Zhang, S.; Yan, J.; Qi, H.; Luan, J.; Qiao, W.; Li, Z. *Pet. Sci. Eng.* **2005**, *47*, 117.
29. Zhao, P.; Howes, A.; Dwarakanath, V.; Thach, S.; Malik, T.; Jackson, A.; Karazincir, O.; Campbell, C.; Waite, J. Presented at the SPE Improved Oil Recovery Symposium, Tulsa, OK, **2010**.
30. Chen, H.; Han, L. J.; Luo, P. Y.; Ye, Z. B. *Surf. Sci.* **2004**, *552*, 53.
31. Rosen, M. J.; Wang, H.; Shen, P.; Zhu, Y. *Langmuir* **2005**, *21*, 3749.
32. Qiu, L. G.; Xie, A. J.; Shen, Y. H. *Mater. Chem. Phys.* **2005**, *91*, 269.
33. Dai, Y. H.; Wu, F. P.; Li, M. Z.; Wang, E. J. *Acta Chim. Sinica* **2005**, *63*, 1329.
34. Wang, Y.; Lu, D.; Long, C.; Han, B.; Yan, H. *Langmuir* **1998**, *14*, 2050.
35. Talwar, S.; Scanu, L.; Raghavan, S. R.; Khan, S. A. *Langmuir* **2008**, *24*, 7797.
36. Hashidzume, A.; Mizusaki, M.; Yoda, K.; Morishima, Y. *Langmuir* **1999**, *15*, 4276.
37. Chen, H.; Han, L. J.; Xu, P.; Luo, P. Y. *Acta Physicochim. Sinica* **2003**, *19*, 1020.
38. Chen, H. Chin. Pat. 1,013,573,07B (**2010**).
39. Abe, M.; Tsubone, K.; Koike, T.; Tsuchiya, K.; Ohkubo, T.; Sakai, H. *Langmuir* **2006**, *22*, 8293.
40. Tikariha, D.; Ghosh, K. K.; Quagliotto, P.; Ghosh, S. *J. Chem. Eng. Data* **2010**, *55*, 4162.
41. Shang, Y.; Wang, T. F.; Han, X.; Peng, C. J.; Liu, H. L. *Ind. Eng. Chem. Res.* **2010**, *49*, 8852.
42. Hourdet, D.; Gadgil, J.; Podhajecka, K.; Badiger, M. V.; Brulet, A.; Wadgaonkar, P. P. *Macromolecules* **2005**, *38*, 8512.
43. Yahaya, G. O.; Ahdab, A. A.; Ali, S. A.; Abu-Sharkh, B. F.; Hamad, E. Z. *Polymer* **2001**, *42*, 3363.
44. Hou, Z.; Li, Z.; Wang, H. *Colloids Surf. A* **2000**; *166*, 243.
45. Akiyama, E.; Kashimoto, A.; Hotta, H.; Kitsuki, T. *Colloid Interface Sci.* **2006**, *300*, 141.
46. Petrovic, L. B.; Sovilj, V. J.; Katona, J. M.; Milanovic, J. L. *Colloid Interface Sci.* **2010**, *342*, 333.
47. Hill, A.; Candau, F.; Selb, J. *Prog. Colloid Polym. Sci.* **1991**, *84*, 61.
48. Zhu, Y. J.; Zhang, J. *J Southwest Pet. Univ. Sci. Technol. Ed.* **2010**, *32*, 131.

49. Han, M.; Zhou, X.; Alhasan, F. B.; Zahrani, B.; AlSofi, A. M. Presented at the SPE EOR Conference at Oil and Gas West Asia, Muscat, Oman, April **2012**.
50. Song, W.; Zeng, X.; Yao, H.; Li, J.; Lv, X.; Tian, Y.; Guo, Y. Presented at the SPE Asia Pacific Oil and Gas Conference and Exhibition, Melbourne, Australia, Oct **2002**.
51. Yue, X. A.; Hou, J. R.; Lv, X.; Zhang, L. J. *Oilfield Chem.* **2008**, *25*, 904.
52. Zhang, H.; Dong, M.; Zhao, S. *Energy Fuels* **2010**, *24*, 1829.
53. Chen, Z. H.; Li, H. B.; Cao, B. G. *Offshore Oil* **2005**, *25*, 53.